An analysis of cross-sections of ^{9}Be $+^{28}$Si interaction in the framework of the double-folding model

A.M. Kabyshev[*,1], K.A. Kuterbekov[1], A.K. Azhibekov[1], K.Zh. Bekmyrza[1], A.M. Mukhambetzhan[2], M.K. Kenzhebek[1], Ye.K. Sovetkhanov[1], Zh.A. Yeltay[1]

[1]L.N. Gumilyov Eurasian National University, Astana, Kazakhstan

[2]Korkyt-Ata Kyzylorda State University, Kyzylorda, Kazakhstan

E-mail: assetenu@gmail.com

In this paper the experimental data on the differential cross sections for elastic scattering of ^{9}Be ions on ^{28}Si nucleus at the energies of the incident nucleus ranging from 12 to 201.6 MeV were analyzed in the framework of the double-folding model using the Paris NN-potential CDM3Y. A good agreement with the experimental angular distributions of differential cross sections for elastic scattering was obtained and the values of the total reaction cross sections were calculated. When the double-folding potential was used as real and imaginary parts, no manifestation of the threshold anomaly was detected. The reason for such a behavior of the potential can be explained by the presence of break-up and/or transfer channels at low energies.

Keywords: weakly-bound nuclei, threshold anomaly, angular distributions of differential cross sections, total reaction cross sections, double-folding potential.

Introduction

It was found that a decrease in the energy of incident particles, i.e. a decrease in the number of open channels, must cause a reduction in the imaginary part of the potential and its vanishing at energies close to the Coulomb barrier. This phenomenon is called a threshold anomaly [1, 2].

However, for weakly-bound nuclei the situation is quite different. In systems where a weakly-bound nucleus interacts with a nucleus of the target, there is a strong connection between the elastic scattering channel and other channels (break-up or transfer of nucleons) [3]. In this case, due to the presence of these additional channels, the reaction has a large cross section and, hence, the imaginary part of the potential cannot decrease and tend to zero with decreasing energy.

An analysis of the experimental results aimed at studying of elastic and inelastic scattering of nuclei - the processes most sensitive to the geometric dimensions of the nuclei (the density distribution of nucleons in the nucleus) and their potential interactions - as a rule, uses both macroscopic and microscopic approaches. To obtain information about the nucleus structure it is necessary to gain a detailed knowledge of the mechanism of nucleus-nucleus interaction, which includes construction of nucleus-nucleus optical potentials.

The problem of ambiguity of potential parameters is a typical problem for macroscopic optical potentials obtained from the analysis of differential cross sections for elastic scattering. The microscopic models will enable us to avoid the use of phenomenological parameters and advance in the description of the properties of atomic nuclei.

Firstly, the model takes into account the structural description of the nucleus (the matter density distribution), secondly, the nucleon-nucleon potential takes into account interaction at the microscopic level and depends on the density of nucleons within the nucleus. In such models the real part of the potential is usually calculated on the basis of the double-folding model, whereas the imaginary part remains phenomenological and is chosen in the Woods-Saxon form.

For ^{6}Li nucleus the threshold energy of ($\alpha + d$) break-up 1.48 MeV with no lower bound excited states. For scattering of this nucleus on ^{208}Pb, ^{138}Ba and ^{28}Si the threshold anomaly is not observed [4-7]. However, for ^{7}Li nuclei scattered by the nuclei of the same targets, a threshold anomaly is detected [4, 5, 7, 8]. The difference between these two lithium isotopes is that ^{6}Li has a high threshold energy of ($\alpha + t$) break-up equal to 2.47 MeV and one bound excited state ($J^\pi = 1/2^-$) at an energy of 0.48 MeV.

^{9}Be nucleus is a loosely bound cluster with a small binding energy of a neutron (1.665 MeV) and an alpha-particle (2.55 MeV). ^{9}Be has no bound excited states at energies lower than 1.665 MeV. Therefore, interaction of ^{9}Be with ^{28}Si must have specific features mentioned above.

Investigations of ^{9}Be scattering gave contradictory results. In the experiments on scattering of ^{9}Be on ^{27}Al nuclei at 12-47 MeV [9], on ^{64}Zn nuclei at 17-28 MeV [10, 11] and on ^{209}Bi nuclei at 35-50 MeV [12, 13] no threshold anomaly was discovered, whereas scattering of ^{9}Be nucleus on ^{208}Pb nucleus [14] showed such an anomaly.

In this paper we present the results of a joint analysis of angular distributions of differential and total reaction cross sections (σ_R) for the ^{9}Be+ ^{28}Si interaction in the framework of the double-folding model, in which the imaginary part of the potential is obtained on the microscopic basis.

Analysis of the Experimental Data

Differential cross sections for elastic scattering of ^{9}Be on ^{28}Si nucleus were obtained using the potential calculated by the DFM-POT program [15], on the basis of the double-folding model.

The potential of interaction of two colliding nuclei in the first order in effective forces can be written as:

$$V^{DF} = V^D + V^{EX}, \tag{1}$$

$$V^D(r) = \int d^3r_p d^3r_t \rho_p(r_p)\rho_t(r_t)v^D_{NN}(s), \tag{2}$$

$$s = r + r_t - r_p, \tag{3}$$

$$V^{EX}(r) = \int d^3r_p d^3r_t \rho_p(r_p, r_p + s)\rho_t(r_t, r_t - s)v^{EX}_{NN}(s)\exp(ik(r)s/\mu), \tag{4}$$

where V^D is the potential of direct folding, V^{EX} is the potential taking into account the nucleon exchange, $\rho_{p,t}$ are density distributions for the incident nucleus and the target nucleus, respectively, $k(R)$ is a local momentum of the relative motion of the nuclei, defined by the relation.

$$k^2(r) = (2m\mu/h^2)[E - U(R) - V_C(R)], \tag{5}$$

where $\mu = A_1 A_2/(A_1 + A_2)$, E is the energy in the center-of-mass system, and $V_C(R)$ is the Coulomb potential.

There are several types of potentials of effective nucleon-nucleon forces v_{NN}. We used the Paris potential CDM3Y [16], which has the following form:

$$v(E, \rho, s) = g(E)F(\rho)v(s), \tag{6}$$

$$g(E) = 1 - 0.003E/A_p, \tag{7}$$

$$F(\rho) = C[1 + \alpha \exp(-\beta\rho) - \gamma\rho], \tag{8}$$

$$v(s) = \sum_{i=1,2,3} N_i \frac{\exp(-\mu_i s)}{\mu_i s}, \tag{9}$$

$$\rho = \rho_p + \rho_t, \tag{10}$$

with the following parameters $C = 0.2658$, $\alpha = 3.8033$, $\beta = 1.4099$, $\gamma = 4.0$.

The density distribution for the incident ^{9}Be nucleus was taken from [17]:

$$\rho(r) = (A + BC^2r^2)\exp(-C^2r^2) + (D + EF^2r^2)\exp(-F^2r^2), \tag{11}$$

where $A = 0.0651$, $B = 0.0398$, $C = 0.5580$, $D = 0.0544$, $E = 0.0332$ and $F = 0.4878$. The root-mean-square radius of ^{9}Be nucleus for this configuration is 2.73fm.

As the density distribution function in the target nucleus ^{28}Si, we used the function of a harmonic oscillator with a standard radius of 3.138 fm, taken from [18]:

$$\rho(r) = 0.205(1 + 0.1941r^2)\exp(-0.2112r^2), \tag{12}$$

Figure 1 shows the matter density distributions for ^{9}Be and ^{28}Si nuclei, which we used in our calculations.
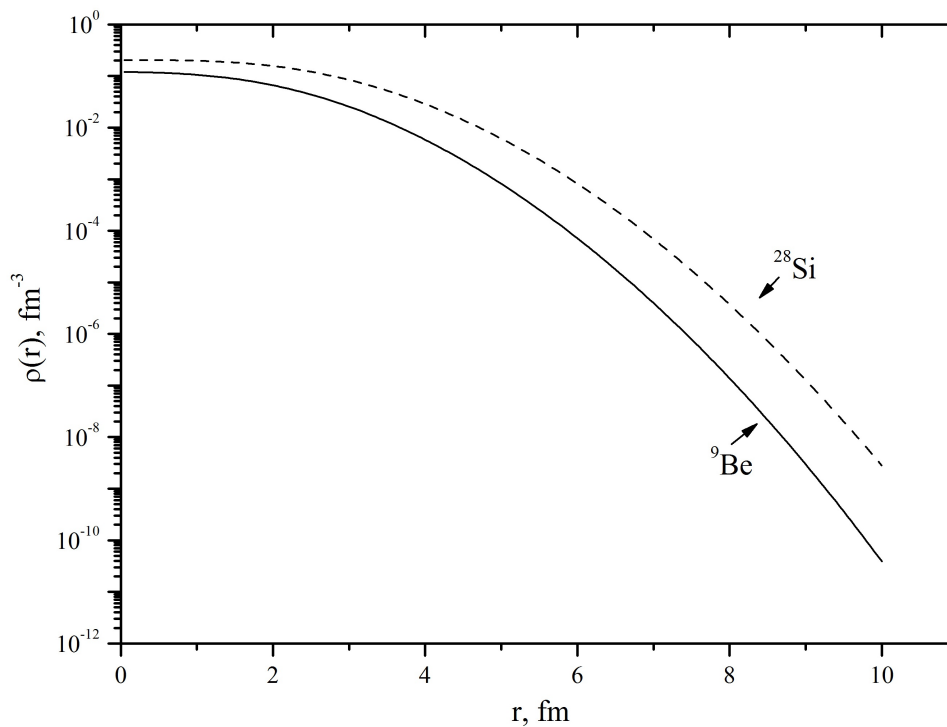

Figure 1. The matter density distributions for ^{9}Be and ^{28}Si nuclei.

The total optical potential usually consists of the real and imaginary parts. In our case, it was assumed that the imaginary part of the potential has the same radial shape as the real part and we use the same double-folding potential, but with a different normalization factor.

$$U(r) = N_r V^{DF}(r) + iN_w V^{DF}(r) + V_C(r), \tag{13}$$

where $N_{r,w}$ are factors normalizing the depth of the real and imaginary parts, respectively, which varied in order to get the best fit with the experimental data on the differential cross sections and the total reaction cross sections. The last term $V_C(r)$ in (13) is the Coulomb potential, which is assumed to have the form of a uniformly charged sphere of a radius $R_C = 1.25(A_p^{1/3} + A_t^{1/3})$, where A_p and A_t are mass numbers of the projectile nucleus and the target nucleus, respectively.

The code FRESCO has been used for the calculations [19]. Parameters N_r and N_w, giving the best correspondence between the experimental and theoretical values of cross sections were found by the minimization of the quantity:

$$\chi^2 = \frac{1}{N_{exp}} \sum_{i=1}^{N_{exp}} [\frac{\sigma^{theor}(\theta_i) - \sigma^{exp}(\theta_i)}{\Delta\sigma^{exp}(\theta_i)}]^2, \tag{14}$$

where N_{exp} is the number of experimental points in the angular distribution, σ^{theor} and σ^{exp} are calculated and measured values of the differential scattering cross section at an angle θ_i, and $\Delta\sigma^{exp}$ is the uncertainty of $\sigma^{exp}(\theta_i)$.

The optimal parameters of the double-folding potential for elastic scattering of ^{9}Be on ^{28}Si nucleus, the values of χ^2/N and the values of the volume integrals of real J_v and imaginary J_w parts of potentials are presented in Table 1.

Table 1 shows that the values of normalizing factors N_r and N_w are in the range 0.350-0.600 [1, 4, 7, 20, 21, 22], it was shown that in order to get optimal description of the experimental data, in the double-folding potential for the interaction of weakly-bound nuclei it is necessary to reduce the depth of the potential by about 60 %.

It should be noted that for ^{9}Be scattering the ratio of parameters is $N_r/N_w \approx$ 1.5, which is similar to the case of ^{6,7}Li scattering.

Table 1 presents the values of the real and imaginary parts of the volume integrals of the potential. As is known, the volume integrals of different potential families differ considerably because of discrete ambiguity, but have the same order of magnitude for different types of charged particles, and there are potential families with the same value of $J_{v,w}/A_pA_t$ for different types of incident particles scattered by the same nuclei. We used potential families with J_v/A_pA_t = 145-224 MeVfm^3 and J_w/A_pA_t = 145 - 282 MeVfm^3. The table also gives χ^2/N values, which, as it is seen, are within the permissible limit.

Figure 2 and Figure 5 shows the results of analysis of angular distributions of differential cross sections for elastic scattering of ^{9}Be on ^{28}Si nucleus with potential parameters from Table 1. The figures show a good description of the experimental data in the entire angular range.

The Coulomb barrier for the ^{9}Be+ ^{28}Si interaction is 14.45 MeV in the laboratory system. Therefore, in the angular distributions for elastic scattering at 12, 13 and 14 MeV, Rutherford scattering prevails up to 60°, and parameters used to describe the experimental data at these energies are not sensitive to the nuclear potential.

Figure 6 shows the real and imaginary parts of the renormalized potential $U = 0.485V^{DF} + i0.544V^{DF}$, obtained for the elastic scattering of ^{9}Be on ^{28}Si at an energy of 30 MeV. As seen from Figure 6, the direct and exchange parts of the potential have different signs: the direct part of the potential has a plus sign and is repulsive, whereas the exchange part is attracting. The total potential is repulsive.

For elastic scattering of ^{9}Be on ^{28}Si nucleus at other energies, the potentials have a shape (radius and diffuseness) similar to that shown in Figure 6, but differ in depth and normalization coefficients N_r and N_w. Therefore, as can be seen from Table 1, the RMS values of potential radii are practically the same for the whole energy range.

Figure 7 shows the energy dependence of the normalizing factors N_r and N_w. It is seen that the depth of the real part for the energies near the Coulomb barrier and higher (12-201.6 MeV) is practically independent of energy. The behavior of

Table 1.
Optical potential parameters.

| Energy (MeV)	N_r	N_w	J_v/A_pA_t (MeVfm^3)	J_w/A_pA_t (MeVfm^3)	$\langle r^2\rangle_r^{1/2}$ (fm)	$\langle r^2\rangle_w^{1/2}$ (fm)	σ_r (mb)	χ^2/N
12	0.400	0.605	186.222	281.660	4.651	4.651	276.8	0.204
13	0.400	0.605	186.060	281.415	4.651	4.651	430.4	0.183
14	0.400	0.605	185.898	281.170	4.651	4.651	576.1	0.630
17	0.400	0.605	185.413	280.437	4.651	4.651	921.7	0.328
20	0.400	0.402	184.929	185.853	4.651	4.651	1092	2.799
23	0.485	0.544	223.641	250.847	4.651	4.651	1327	2.271
26	0.485	0.544	223.058	250.193	4.651	4.651	1449	1.140
30	0.485	0.544	222.282	249.322	4.651	4.651	1568	5.192
50	0.400	0.494	180.161	222.500	4.652	4.652	1794	3.908
121	0.346	0.377	146.506	159.633	4.655	4.655	1810	12.574
201.6	0.369	0.368	145.671	145.276	4.660	4.660	1755	9.651
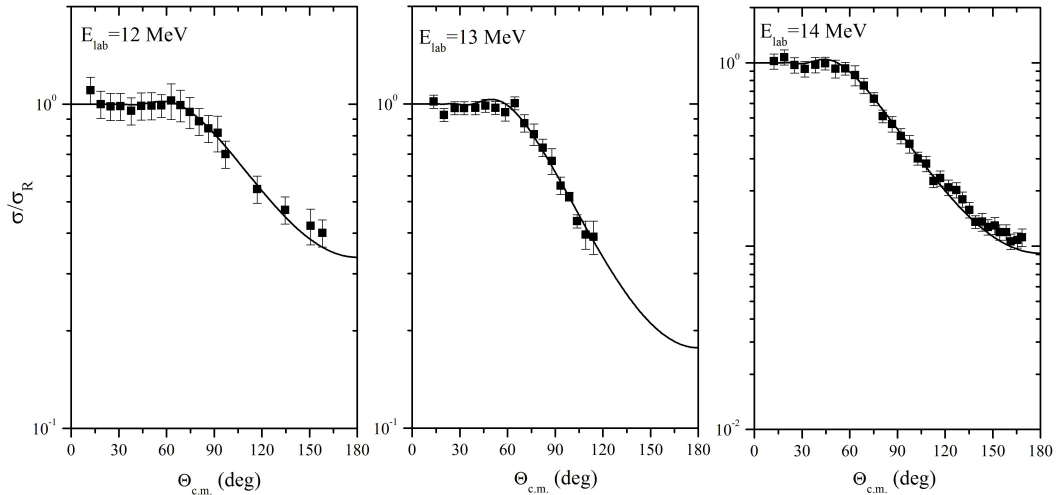
Figure 2. The elastic scattering angular distributions for ^{9}Be+ ^{28}Si at different energies. Points are the experimental data [23, 24], the solid line is the result of calculations using the double-folding potential with the parameters from Table 1.
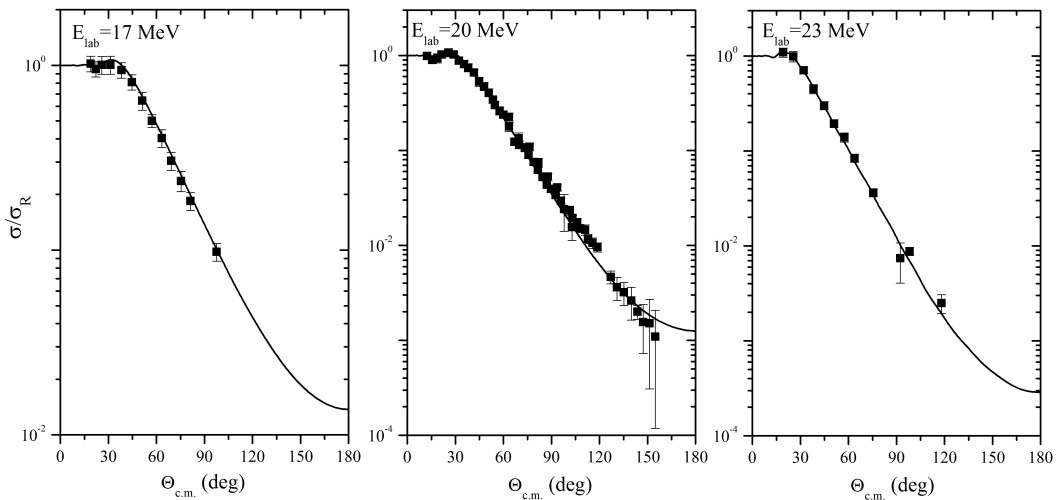

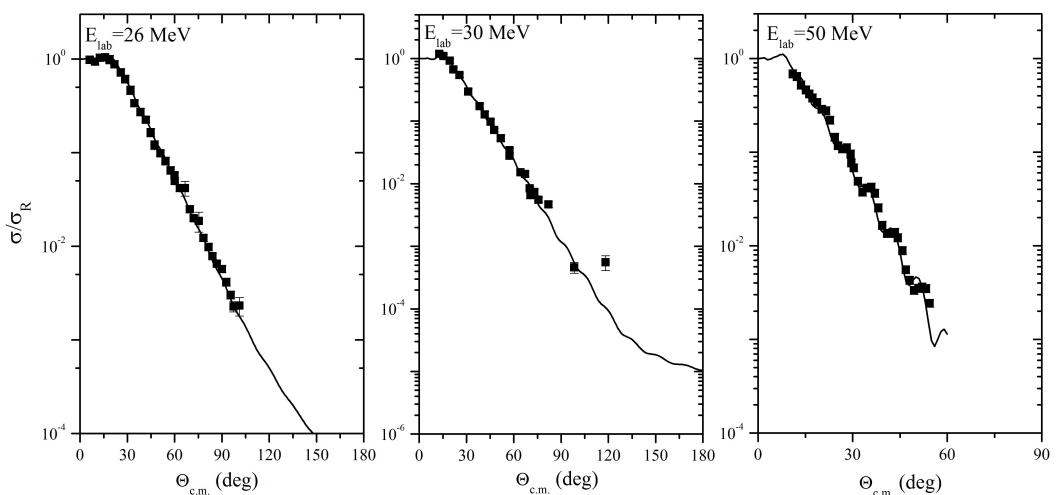Figure 3. Same as Figure 2, but for the energies 17, 20 and 23 MeV.

Figure 4. Same as Figure 2, but for the energies 26, 30 and 50 MeV.

the imaginary part is different from that of the real part: even at energies below the Coulomb barrier and close to it (12-30 MeV) - the depth of the potential increases and then gradually decreases with increasing energy. This behavior of the potential
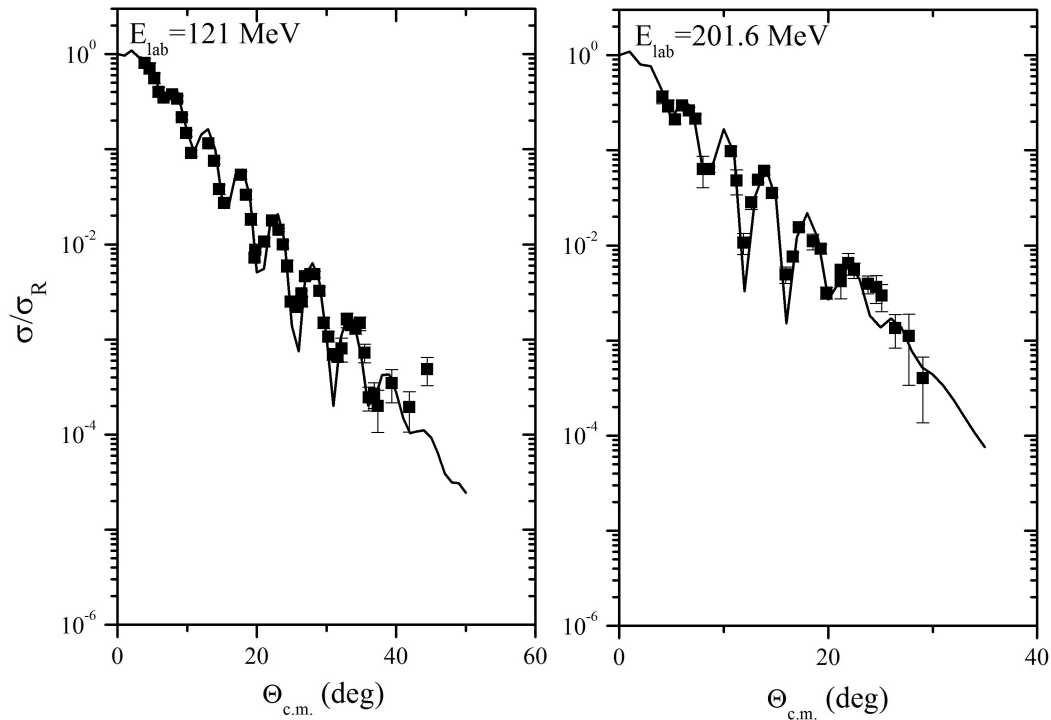
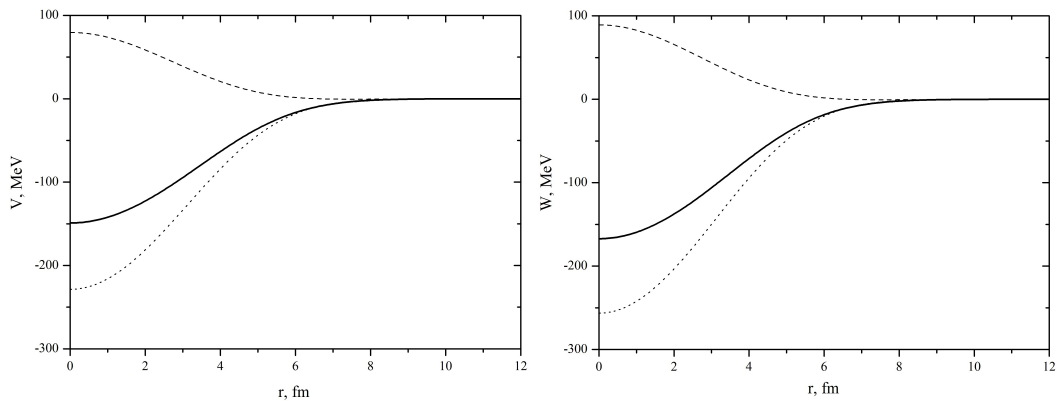Figure 5. Same as Figure 2, but for the energies 121 and 201.6 MeV.

Figure 6. The real (left) and the imaginary (right) parts of the potential for the ^{9}Be + ^{28}Si elastic scattering at an energy of 30 MeV. The dashed line is a direct part of the potential V^D, the dotted line is the exchange part of the potential V^{EX}, the solid line is the total potential $V^{DF} = V^D + V^{EX}$.

shows that there is no threshold anomaly for the ^{9}Be+^{28}Si reaction in this energy range.

This is confirmed by the following conclusions. For the ^{9}Be+^{28}Si system there are open channels of reactions at energies below and near the Coulomb barrier (12 - 30 MeV), which is why the imaginary part of the potential does not approach zero at these energies.

^{9}Be is a cluster weakly-bound nucleus (^{8}Be $+ n$ - S_n = 1.665 MeV, ^{5}He+ ^{4}He - S_α = 2.55 MeV) and does not have any bound excited states below 1.665 MeV, and therefore, in reactions with its participation, the reaction cross section at sub-barrier energies must increase. The most probable reaction channels for this system are break-up of the nucleus and transfer of the nucleon.

Angular distributions of differential cross sections for elastic scattering of ^{9}Be on ^{28}Si nucleus were used to calculate σ_R. Figure 8 shows the experimental data
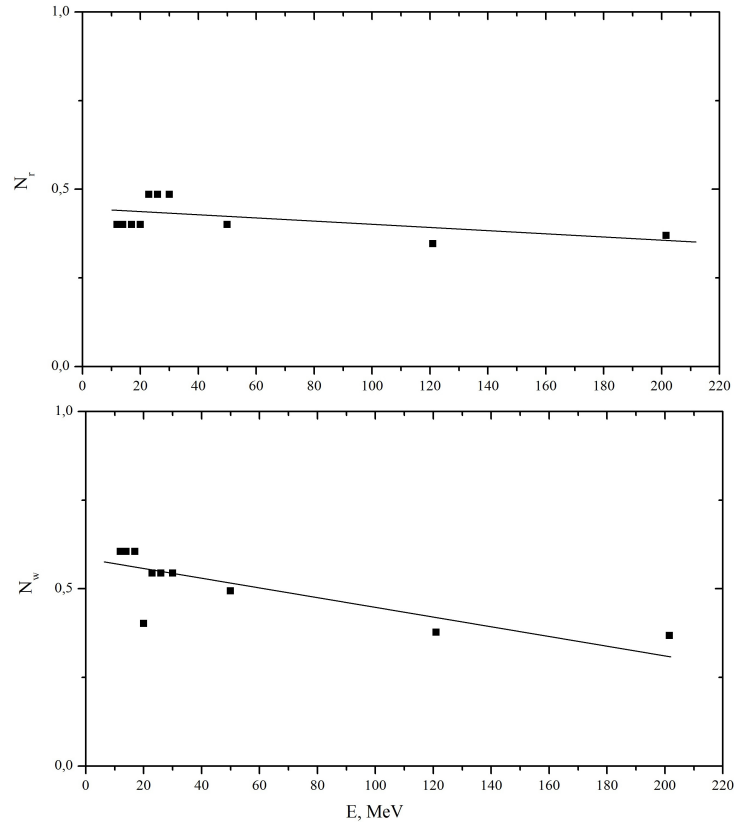
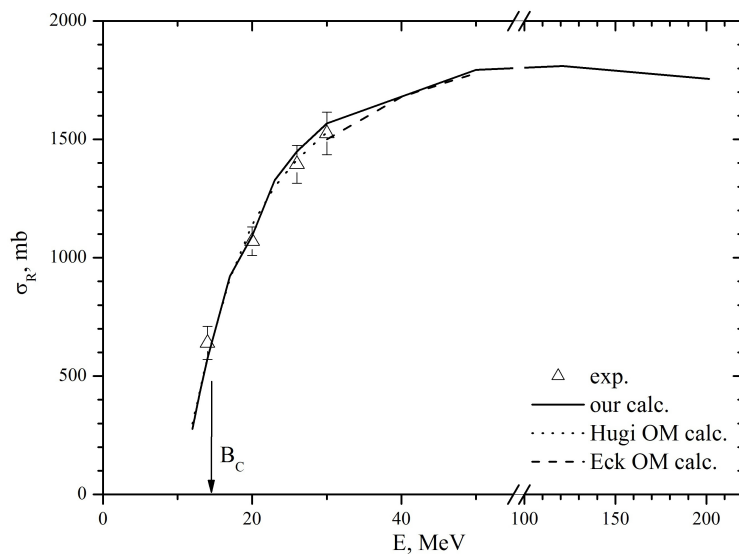Figure 7. The dependence of N_r and N_w on the energy of the incident nucleus.

Figure 8. Total reaction cross sections for the ^{9}Be+^{28}Si interaction. $\triangle$ denotes the experimental data [26]. The solid line is the result of calculation using the double-folding potential with parameters from Table 1. The dotted line is the result of calculations by the optical model [23], the dashed line is the result of calculations by the optical model [25]. The arrow shows the Coulomb barrier of the reaction.

on σ_R for ^{9}Be+^{28}Si interaction at the energies of the incident nucleus ranging from 12 to 201.6 MeV, as well as σ_R values, calculated in this work and the results of calculations made in [23, 25] in the framework of the optical model using the Woods-Saxon potential.

Figure 8 shows that at energies close to the Coulomb barrier (12-20 MeV), σ_R increases with an increase in the amount of energy. This confirms the fact that

there are open reaction channels in this energy range.

It is seen that the results of our calculations are in good agreement with the experimental and earlier calculated values of σ_R.

Conclusion

The experimental data on the differential cross sections for elastic scattering of ^{9}Be ions on ^{28}Si nucleus at energies of the incident nucleus ranging from 12 to 201.6 MeV were analyzed in the framework of the double-folding model with the Paris NN-potential CDM3Y.

A significant difference between the behavior of the real and imaginary parts of the potential was revealed: the depth of the real part remains constant and is almost independent of energy at energies higher than the sub-barrier energies, whereas the depth of the imaginary part increases at energies below and near the Coulomb barrier (12-30 MeV) and then gradually decreases with increasing energy. This behavior of the potential shows the absence of the threshold anomaly, which is caused by the presence of break-up and transfer channels at the energies below and near the Coulomb barrier.

The energy dependence of the total reaction cross section for the ^{9}Be+^{28}Si interaction was determined and compared with the available experimental and theoretical data.

It should be noted that in this paper the real and imaginary parts of the optical potential were obtained only on the microscopic base. This approach allowed us to get a good description of the experimental data on the differential and total reaction cross sections for the ^{9}Be+^{28}Si interaction.

These parameters of the potential, describing the experimental data on elastic scattering and total reaction cross sections, make it possible to state that the calculated values of potential parameters are realistic.

References

[1] G.R. Satchler, Phys. Rep. **199** (1991) 147.
[2] G.R. Satchler and W. Love, Phys. Rep. **55** (1979) 183.
[3] C. Mahaux et al., Nucl. Phys. A **55** (1986) 354.
[4] N. Keeley et al., Nucl. Phys. A **571** (1994) 326.
[5] A.M. Maciel et al., Phys. Rev. C **59** (1999) 2103.
[6] A. Pakou et al., Phys. Lett. B **556** (2003) 21.
[7] M.A. Tiede et al., Phys. Rev. C **44** (1991) 1698.
[8] A. Pakou et al., Phys. Rev. C **69** (2004) 054602.
[9] P.R.S. Gomes et al., Phys. Rev. C **70** (2004) 054605.
[10] S.B. Moraes et al., Phys. Rev. C **61** (2000) 064608.
[11] P.R.S. Gomes et al., Heavy Ion Phys. **11** (2000) 361.
[12] C. Signorini, Eur. Phys. J. A **13** (2002) 129.
[13] C. Signorini et al., Nucl. Phys. A **701** (2002) 23.
[14] R.J. Wooliscroft et al., Phys. Rev. C **69** (2004) 044612.

[15] K.V. Lukyanov et al., Bull. Rus. Acad. Sci. Phys. **72** (2008) 382.

[16] D.T. Khoa, G.R. Satchler, Nucl. Phys. A **668** (2000) 3.

[17] V. Hnizdo et al., Phys. Rev. C **24** (1981) 1495.

[18] O.M. Knyazkov, E.F. Hefter, Z. Phys. A **301** (1981) 277.

[19] I.J. Thompson, Comput. Phys. Rep. **7** (1988) 167.

[20] M.E. Brandan, G.R. Satchler, Phys. Rep. **285** (1997) 143.

[21] Y. Sakuragi et al., Prog. Theor. Phys. **70** (1983) 1047.

[22] L. Trache et al., Phys. Rev. C **61** (2000) 024612.

[23] M. Hugi et al., Nucl. Phys. A **368** (1981) 173.

[24] M.S. Zisman et al., Phys. Rev. C **21** (1980) 2398.

[25] J.S. Eck et al., Phys. Rev. C **21** (1980) 2352.

[26] Yu.A. Pozdnyakov, Phys. Atomic Nuclei **65** (2002) 1827.